ACS APPLIED MATERIALS & INTERFACES

Research Article

www.acsami.org

Facile Preparation of Monodisperse, Impurity-Free, and Antioxidation Copper Nanoparticles on a Large Scale for Application in Conductive Ink

Yu Zhang,[†,‡,§] Pengli Zhu,[*,†,∥] Gang Li,[†] Tao Zhao,[†] Xianzhu Fu,[†] Rong Sun,[*,†] Feng Zhou,[‡] and Ching-ping Wong[∥,⊥]

[†]Shenzhen Institutes of Advanced Technology, Chinese Academy of Sciences, Shenzhen, China

[‡]State Key Laboratory of Solid Lubrication, Lanzhou Institute of Chemical Physics, Chinese Academy of Sciences, Lanzhou, China

[§]Graduate School of the Chinese Academy of Sciences, Beijing, China

[∥]School of Materials Science and Engineering, Georgia Institute of Technology, Atlanta, Georgia 30332-0245, United States

[⊥]Department of Electronics Engineering, The Chinese University of Hong Kong, Hong Kong, China

ABSTRACT: Monodisperse copper nanoparticles with high purity and antioxidation properties are synthesized quickly (only 5 min) on a large scale (multigram amounts) by a modified polyol process using slightly soluble $Cu(OH)_2$ as the precursor, L-ascorbic acid as the reductant, and PEG-2000 as the protectant. The resulting copper nanoparticles have a size distribution of 135 ± 30 nm and do not suffer significant oxidation even after being stored for 30 days under ambient conditions. The copper nanoparticles can be well-dispersed in an oil-based ink, which can be silk-screen printed onto flexible substrates and then converted into conductive patterns after heat treatment. An optimal electrical resistivity of 15.8 $\mu\Omega$ cm is achieved, which is only 10 times larger than that of bulk copper. The synthesized copper nanoparticles could be considered as a cheap and effective material for printed electronics.

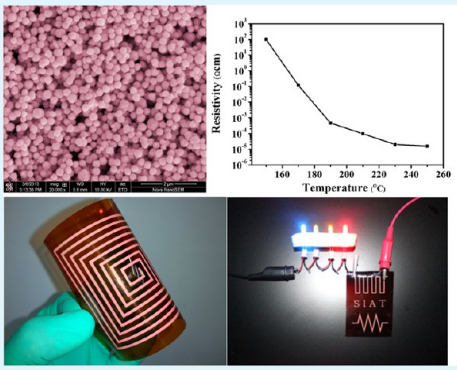

KEYWORDS: *copper nanoparticles, monodisperse, antioxidative, large scale, flexible conductors*

1. INTRODUCTION

Recently, there has been growing interest in using printed electronic technology to make cost-effective and eco-friendly electronic devices, such as solar cells, integrated circuits, radiofrequency identification (RFID), organic light-emitting diodes (OLEDs), and printed circuit boards (PCBs).[1,2] Conductive ink that can be patterned by silk-screen printing, inkjet printing, or an other printing process to form conductive tracks[3,4] is a critical component of printing electronic technology in achieving conductive patterns with a high degree of uniformity and electrical conductivity.[5,6] Metal nanoparticles that possess high conductivity and operational stability are considered as the key constituents for preparing the conductive ink. In this context, the synthesis of desirable metal nanoparticles via a facile approach and in a large quantity for application in conductive ink has been a challenge.

With regard to the choice of metal nanomaterial, most recently relevant studies have focused on silver and gold nanoparticles because of their high conductivity and strong antioxidation properties.[7−9] However, they are rather unsuitable for practical use because of the high cost of gold nanoparticles and the low resistivity toward ion migration of silver nanoparticles. Therefore, we sought an alternative that is inexpensive, highly conductive, and stable in air. Copper, because it possesses a similar electrical resistivity and thermal conductivity, can be a good candidate material in the printed electronics industry because of its lower cost and strong durability toward ion migration.

As such, various methods have been developed to synthesize nanocopper for conductive ink, such as thermal decomposition,[10] the sonochemical method,[11] laser ablation,[12] chemical reduction,[13,14] radiation methods,[15] microemulsion techniques,[16] etc. Among the aforementioned methods, recent research has focused mainly on wet chemical processes that are based on the reduction of copper ions by reducing agents in liquid media.[17,18] This route is convenient because it could result in controllable particle characteristics by regulating experimental variable parameters. Nevertheless, few of the technologies could be practically used, and the problems may be explained as follows. First, in the case of metal nanoparticle-based ink, the oxidation and dispersion instability could be critical problems because rapid oxidation and aggregation might occur because of the high surface:volume ratio of the nanoparticles.[19−21] The tendency of copper nanoparticles to aggregate and oxidize is more pronounced than that of silver or gold. Second, among the commonly used reductants, hydrazine

Received: October 19, 2013
Accepted: December 6, 2013
Published: December 13, 2013

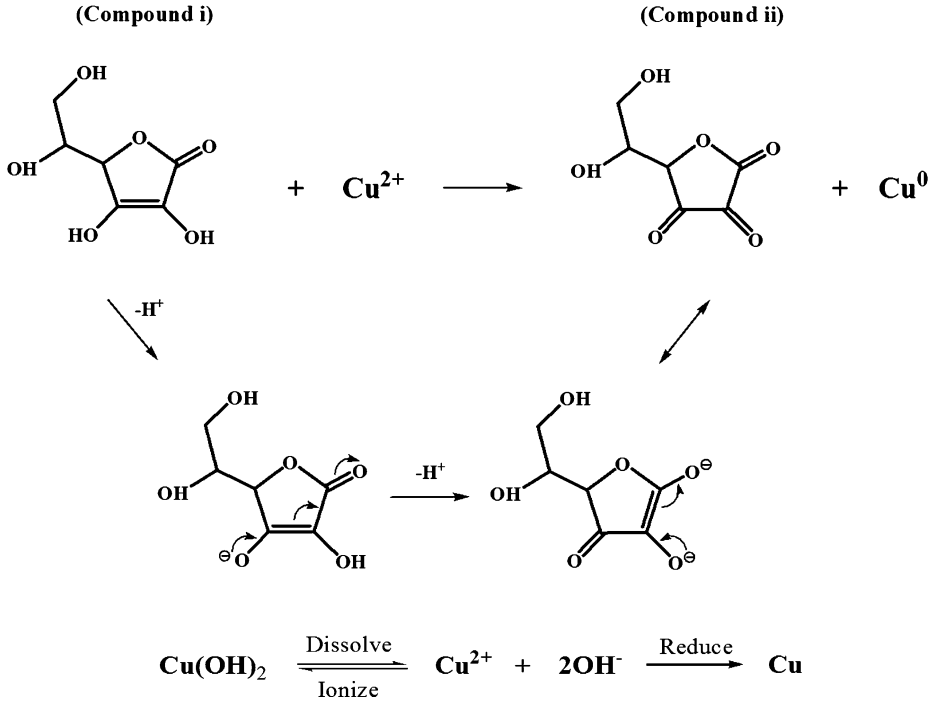

Figure 1. Reaction mechanism of L-ascorbic acid reducing bivalent Cu.

is extremely toxic and dangerous, while sodium borohydride and sodium hypophosphite produce impurities, such as boron and sodium salts, which are hard to remove when samples are washed with solvent. Last but not least is the fact that the synthesis of copper nanoparticles on a gram scale is a prerequisite for application in conductive ink, and such a large quantity synthesis in a short reaction time is desirable because a time-consuming method could cause oxidation.[22] Therefore, it is necessary to coat the copper nanoparticles using dispersing and protective agents to improve the dispersion and also to inhibit oxidation. In the process, nontoxic reductants, minimal postprocessing, and the possibility of mass production are highly desirable.

In this work, we present a convenient, cost-effective, and nontoxic process for synthesizing monodisperse, air-stable, and large-scale copper nanoparticles without complex post-treatment. The copper nanoparticles were prepared using $Cu(OH)_2$ as the copper precursor, L-ascorbic acid as the reducing agent, and PEG-2000 as the protective agent. A conductive ink that can be applied by silk-screen printing was prepared using the copper nanoparticles. The copper conductive ink was printed on a flexible polyimide substrate and annealed into a printed circuit board. Printing and annealing conditions such as ink formulation, silk-screen printing mesh, and annealing temperature were optimized to achieve smooth and continuous conductive tracks with high resolution. In addition, conductivities as a function of annealing temperature were studied, and the microstructures of the annealed patterns were also investigated.

2. EXPERIMENTAL SECTION

2.1. Materials. Copper hydroxide and L-ascorbic acid were purchased from Aladdin reagent Co., Ltd. Ethylene glycol, polyethylene glycol 2000 (PEG-2000), and other ink solvents were purchased from Sinopharm Chemical Reagent Co. Ltd. Deionized water was used in all experiments.

2.2. Preparation of Copper Nanoparticles and Copper-Based Conductive Ink. In a typical preparation process, a $Cu(OH)_2$ polyol solution was prepared by dissolving $Cu(OH)_2$ and PEG-2000 in 40 mL of ethylene glycol. A flask containing a $Cu(OH)_2$ polyol solution was heated to 80 °C in an oil bath while the solution was mechanically stirred for ~0.5 h. Then an L-ascorbic acid polyol solution was heated to 80 °C under the same conditions. The molar ratio of L-ascorbic acid to $Cu(OH)_2$ is 3.4. Then, the latter solution was poured into the former flask, and the obtained mixture was kept at 80 °C for 5 min. Finally, the resulting dispersion was washed four times with ethanol at 8000 rpm for 10 min via centrifugation.

Copper-based conductive ink was formulated by dispersing the synthesized copper nanoparticles into mixed oil solvents that contained ethylene glycol butyl ether, methylcellulose, and other additives. Using this copper-based conductive ink, a printed circuit board was manufactured on a polyimide substrate through silk-screen printing.

2.3. Characterization. The samples were characterized by different techniques. The morphology and size of the synthesized copper nanoparticles were observed with a field-emission scanning electron microscope (FE-SEM, FEI Nova Nano SEM 450). The size distributions of copper nanoparticles were determined with a laser particle analyzer (Malvern ZetasizerNano ZS90). The powder X-ray diffraction (XRD) patterns were recorded on an X-ray diffractometer (Rigaku D/Max 2500) with monochromated Cu Kα radiation (λ = 1.54 Å). X-ray photoelectron spectroscopy (XPS) spectra were recorded on a PHI-5702 multifunctional spectrometer using an Al Kα X-ray excitation source. Fourier transform infrared (FT-IR) spectra were recorded with a Fourier transform infrared spectrophotometer (Vertex70 FT-IR-Spektrometer) between 4000 and 1000 cm^{-1}. Ultraviolet−visible spectroscopy (UV−vis) absorption spectra of the samples were recorded on an UV−vis−NIR spectrometer (Shimadzu UV-3600) with a wavelength range of 300−800 nm. Thermogravimetric (TG) analysis was conducted with a thermogravimetric analyzer (TA Q600). The viscosity and surface tension of copper conductive ink were measured using an Anton Paar MCR302 rheometer and a Dataphysics OCA20 CA meter, respectively. Electrical resistivities of the samples were measured with a Keithly 2410 Source Meter instrument. A Gwinstek programmable linear DC power supply (GPD-3303S) was used as a constant-voltage power source. All measurements were performed at room temperature.

dx.doi.org/10.1021/am404620y | ACS Appl. Mater. Interfaces 2014, 6, 560−567

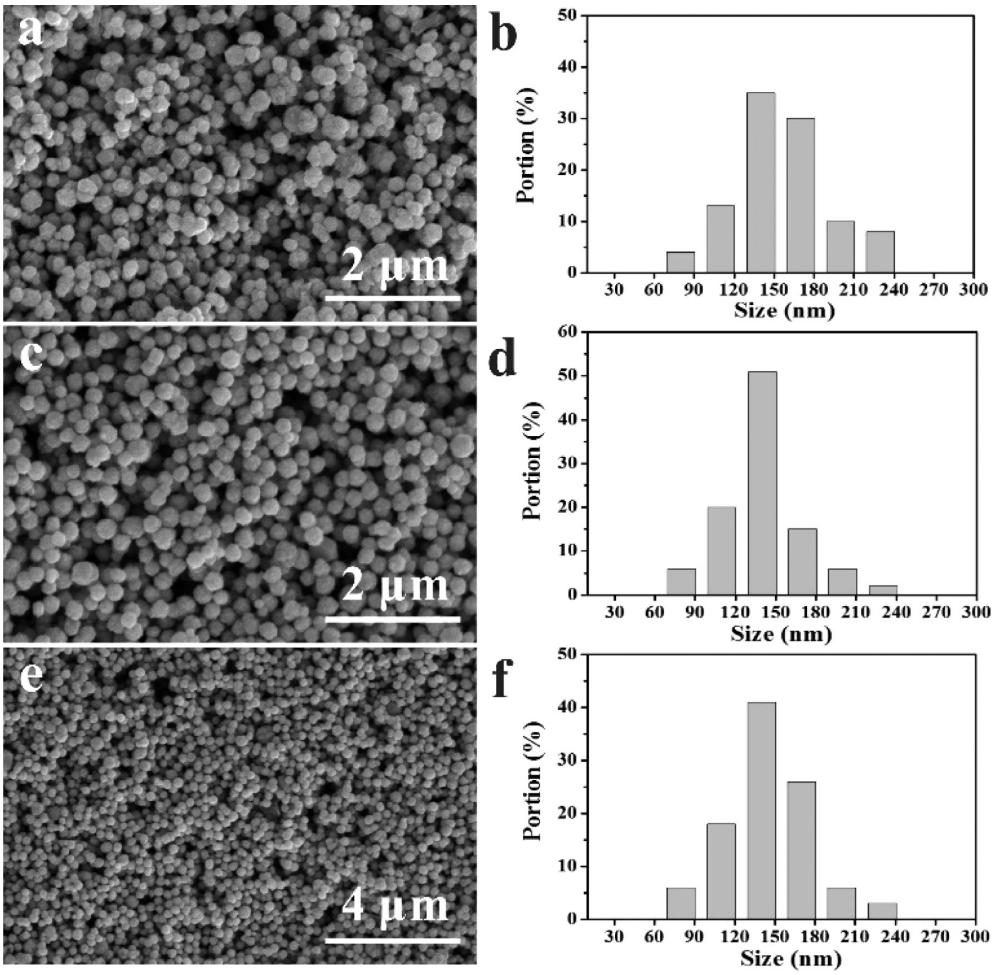

Figure 2. SEM images (a, c, and e) and particle size distributions (b, d, and f) of the as-prepared copper nanoparticles: (a and b) Cu NPs, (c and d) Cu/PEG NPs, and (e and f) scale-up to 0.5 L of Cu/PEG NPs.

3. RESULTS AND DISCUSSION

3.1. Synthesis of Copper Nanoparticles. The mechanism of copper ion reduction by L-ascorbic acid has been described by various reports.[23] In this case, the total reduction process is shown in Figure 1. The structure of L-ascorbic acid (compound **i**) is presented in the top left corner of Figure 1. It behaves as a vinylogous carboxylic acid in which the electrons in the double bond, hydroxyl group lone pair and the lactone ring carbonyl double bond form a conjugated system together. L-Ascorbic acid with a conjugated structure could provide electrons to reduce the bivalent Cu to zerovalent Cu and at the same time itself was oxidized from an enol to the adjacent diketone structure (compound **ii**). To improve our understanding of the nucleation and growth of the copper nanoparticles, this process can be considered as a dynamic procedure between the dissolution and ionization equilibrium of copper hydroxide in the solvent. Copper hydroxide slightly dissolves in the solvent and ionizes to form bivalent copper ions, which are reduced to zerovalent copper instantly. The consumption of Cu^{2+} promotes the dissolution, ionization, and consequent reduction of copper hydroxide. The two equilibria of the three steps (dissolve, ionize, and reduce) determine the growth rate of the copper crystal in the solvent and finally control the particle size and morphology of the nanocopper accordingly. When using L-ascorbic acid as a reducing agent, it could be adsorbed on the surface of copper particles *in situ* through van der Waals force and generate protection from being oxidized. At the same time, oxygen in the L-ascorbic acid molecule that possesses lone pair electrons exhibits coordination with copper particles. Therefore, the protective layer of L-ascorbic acid on the copper surface is formed by the two kinds of forces to achieve the aim of antioxidation. It is worth mentioning that compared with nitric acid copper and other copper salts, copper hydroxide, as a precursor, does not introduce any impurity ions. Furthermore, using L-ascorbic acid as the reductant and polyethylene glycol as the protectant, this procedure is mild, nontoxic, and cost-effective. In addition, the process is easy to scale up, and nearly 6.2 g of copper nanoparticles could be obtained in a 500 mL reaction mixture within 5 min, with a yield of 98%.

3.2. Characteristics of Copper Nanoparticles. The SEM and laser particle analyzer were used to investigate the morphology and size distributions of synthesized copper nanoparticles. Figure 2 shows the morphology and size of the copper particles prepared with $Cu(OH)_2$ as the precursor, in which the left panels are SEM images and the right panels show size distributions. As seen in the figure, without the aid of a protective agent, the prepared copper nanoparticles (Cu NPs) are quasi-spherical with diameters in the range of 162 ± 40 nm (Figure 2a,b). In the presence of protective agent PEG-2000, the obtained copper particles (Cu/PEG NPs) reveal a relatively narrow particle size distribution of 135 ± 30 nm (Figure 2c,d).

dx.doi.org/10.1021/am404620y | ACS Appl. Mater. Interfaces 2014, 6, 560−567

The results suggest that the addition of the polymer protectant efficiently restricts the growth of copper particles. We can thus conclude that PEG-2000 plays an important role in controlling the size of Cu/PEG NPs. Moreover, panels e and f of Figure 2 clearly show that monodisperse copper nanoparticles were also obtained with a higher concentration and larger volume in the scale-up synthesis (500 mL for the starting solution with a concentration of 0.2 mol/L), while the particle morphology and size distribution are both unaffected. Hence, in this cost-effective, time-saving, and eco-friendly system, the slow ionization of cupric hydroxide, weak reducibility of L-ascorbic acid, and protection of PEG-2000 together make it possible to synthesize large-scale monodisperse copper nanoparticles at high concentrations.

The structure of the synthesized copper nanoparticles was determined via XRD. Figure 3a shows the XRD pattern of freshly produced copper nanoparticles with PEG-2000 as the protective agent (Cu/PEG-0 NPs). In the XRD measurement, reflections at 43.47°, 50.67°, and 74.68° are attributed to the (111), (200), and (220) planes of copper, respectively. Therefore, Cu/PEG-0 NPs are confirmed as being phase-pure copper without any impurity phases, such as Cu_2O, CuO, or $Cu(OH)_2$. The sharp and strong peaks also reveal that Cu/PEG-0 NPs are highly crystalline. These characteristic peaks confirm the formation of a face-centered cubic (*fcc*) copper phase (JCPDS No. 04-0836). This indicates that in an extremely short reaction time, the raw material copper hydroxide has completely converted into copper nanoparticles. To study the antioxidative ability of Cu/PEG-0 NPs, XRD characterization was also performed on the same samples after then had been held for 30 days (Cu/PEG-30 NPs), 60 days (Cu/PEG-60 NPs), or 90 days (Cu/PEG-90 NPs) at room temperature under atmospheric pressure without strict conditions like nitrogen protection, etc.; the results are shown in panels b–d of Figure 3, respectively. One can see that the XRD pattern of Cu/PEG-30 NPs exhibits almost the same characteristic peak as that of Cu/PEG-0 NPs. Besides, no characteristic peaks of oxide impurities could be detected. However, the patterns of Cu/PEG-60 NPs and Cu/PEG-90 NPs not only include the characteristics of copper but also exhibit weak reflections at 36.65°, 42.61°, and 61.34°, which are attributed to Cu_2O crystallites (JCPDS No. 34-1354). This suggests that the surface of the copper nanoparticles generated a thin oxide layer after being stored for 60 days. In other words, it indicates that the generation of the copper oxide layer requires at least 30 days, which means the synthesized pure copper nanoparticles could be held for more than a month under ambient conditions. The time-saving and strong

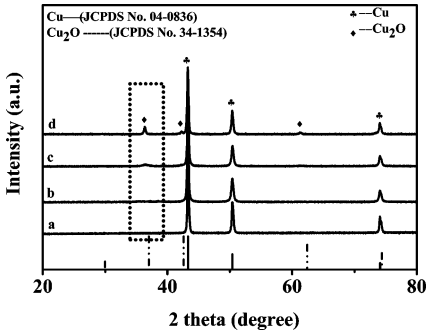

Figure 3. XRD patterns of synthesized copper nanoparticles: (a) Cu/PEG-0 NPs, (b) Cu/PEG-30 NPs, (c) Cu/PEG-60 NPs, and (d) Cu/PEG-90 NPs.

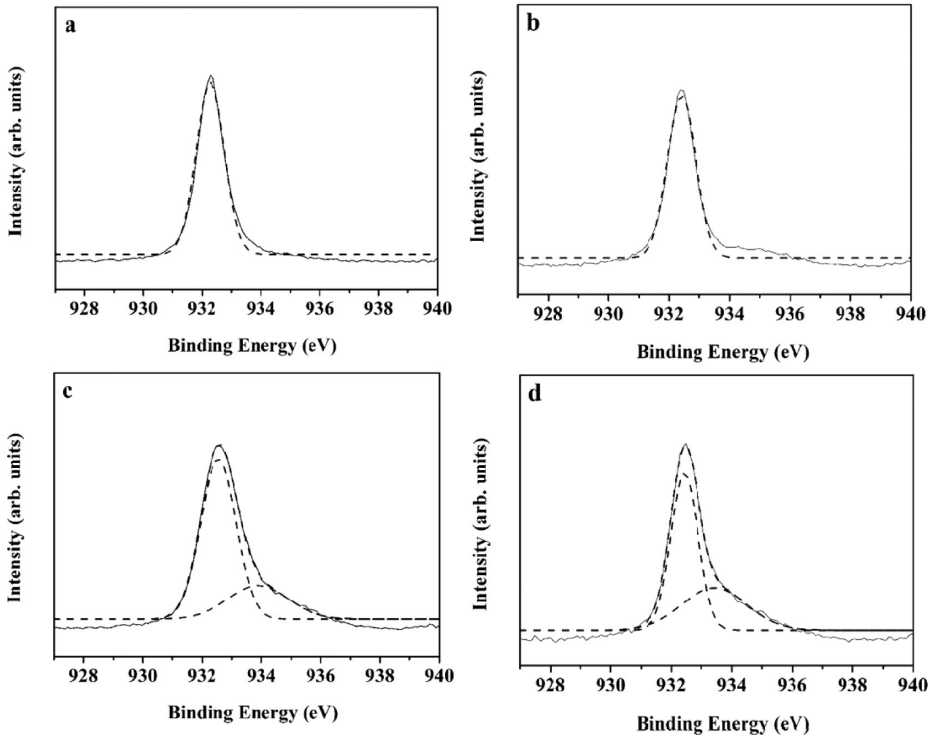

Figure 4. XPS spectra of synthesized copper nanoparticles: (a) Cu/PEG-0 NPs, (b) Cu/PEG-30 NPs, (c) Cu/PEG-60 NPs, and (d) Cu/PEG-90 NPs.

dx.doi.org/10.1021/am404620y | ACS Appl. Mater. Interfaces 2014, 6, 560–567

oxidation resistance of synthesized nanocopper is suitable for conductive ink in printed electronics.

However, XRD is inadequate for analyzing the trace surface oxidation of copper nanoparticles because the surface oxide layer is amorphous and extremely thin. To probe the extent of surface oxidation of copper nanoparticles in depth, XPS analysis was performed. Figure 4 shows the peak fitting of the Cu $2p_{3/2}$ spectra of Cu/PEG NPs at different storage times. As one can see from Figure 4a (0 day), the characteristic Cu $2p_{3/2}$ peak appears at 932.1 eV and no significant peak of CuO appears at 934.0 eV,[24] which indicates Cu/PEG-0 NPs are phase-pure copper without any oxidation layer. In addition, the XPS spectrum of Cu/PEG-30 NPs exhibits almost the same characteristic peak as that of Cu/PEG-0 NPs. The spectra of Cu/PEG-60 NPs and Cu/PEG-90 NPs not only contain the characteristic peaks of $Cu2p_{3/2}$ but also exhibit weak peaks located at 934.0 eV because of the existence of CuO. This suggests that the surface of the synthesized copper nanoparticles would generate a thin oxide layer if the sample were stored for ≥60 days. These results further confirm that the prepared PEG-capped copper nanoparticles could be stored for at least 30 days without any oxidation under ambient conditions.

FT-IR was used to analyze the chemical composition of the copper nanoparticles surface, and spectra of the Cu NPs and Cu/PEG NPs are shown in Figure 5. The characteristic absorptions of hydroxyl at ~3440 cm^{-1} and carbonyl at ~1640 cm^{-1} in curve a are identified, which indicates the synthesized copper nanoparticles are capped with dehydroascorbic acid (compound **ii**) on the surface. The absorptions of hydroxyl and carbonyl are observed for Cu/PEG NPs in curve b, and the differences lie in the bands at 2923, 2850, and 1433 cm^{-1}, which could be assigned to the methylene in polyethylene glycol. This indicates that for Cu/PEG NPs, both dehydroascorbic acid and polyethylene glycol are successfully coated onto the surface of copper nanoparticles, endowing the nanoparticles with antioxidant properties.

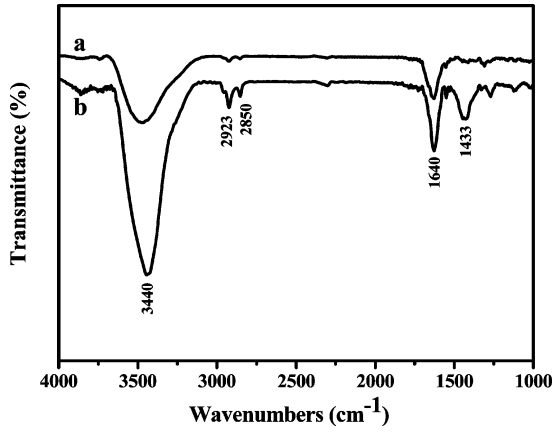

Figure 5. FT-IR spectra of synthesized copper nanoparticles: (a) Cu NPs and (b) Cu/PEG NPs.

Furthermore, the protectant on the surface of copper nanoparticles could be characterized via UV−vis spectroscopy, which has been proved to be a useful technique for studying metal nanoparticles. This is because the peak positions and shapes are sensitive to the particle size of metal nanoparticles and their surface state. The UV−vis absorption spectra of Cu NPs without a protectant are shown in Figure 6a. The first absorption peak is around 330 nm, corresponding to the oxidation product of L-ascorbic acid (compound **ii**), which is shown in Figure 1. The second absorption peak in Figure 6a (0 day) is around 595 nm, corresponding to freshly prepared copper nanoparticles.[25] The absorption peak found for Cu/PEG-30 NPs is shifted to a lower wavelength (red shift), which is possibly due to the oxidation of copper nanoparticles. In contrast, the absorption peak around 590 nm corresponding to copper nanoparticles has nearly no shift after being stored for 30 days (Figure 6b). The almost identical peaks found in Figure 6b can be ascribed to the protective agent on the surface of copper nanoparticles, which has confined their further growth. As one can see from Figure 6, without the aid of a protective agent, the prepared copper nanoparticles are easily oxidized, whereas the copper particles protected by PEG-2000 could be stored for at least one month without any oxidization.

Thermal decomposition behaviors of the synthesized copper nanoparticles were examined by TG analysis. Measurements were performed from room temperature to 800 °C at a rate of 10 °C/min under a nitrogen flow. A nitrogen atmosphere was used for TG measurement to prevent the oxidation of copper, and thus other forms of interference were prevented. As one can see in Figure 7, after equilibrium had been reached, the weight loss of curve a is ~2.47%, which could be attributed to a small amount of water and dehydroascorbic acid adsorbed on the surface of copper nanoparticles. Compared with curve a, curve b finally has a weight loss of ~4.74%. The difference in weight loss between curves a and b is ~2.27%, which might be ascribed to the amount of PEG-2000 coating on the surface of the synthesized copper particles. The results of XRD, XPS, IR, and UV−vis confirmed that PEG-2000 has been successfully

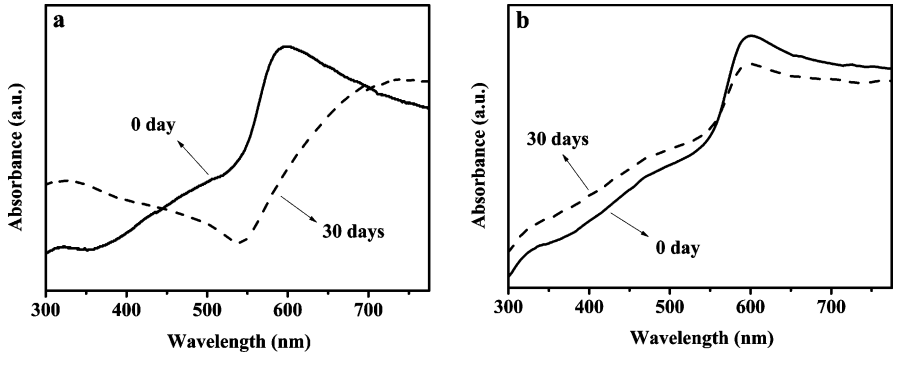

Figure 6. UV−vis absorption spectra of synthesized copper nanoparticles: (a) Cu NPs and (b) Cu/PEG NPs.

dx.doi.org/10.1021/am404620y | ACS Appl. Mater. Interfaces 2014, 6, 560−567

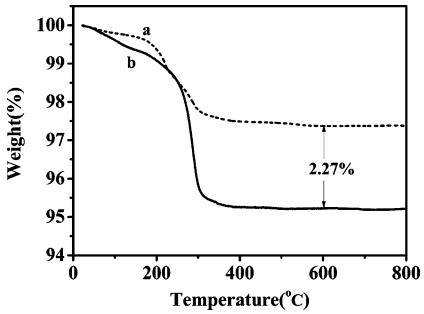

Figure 7. TG results of synthesized copper nanoparticles: (a) Cu NPs and (b) Cu/PEG NPs.

coated on the surface of the as-prepared copper particles, and this small amount of protective agent layer could largely increase the resistance of copper particles to oxidation.

3.3. Thermal and Electrical Properties of the Printed Copper Conductive Patterns. The properties of conductive ink, such as viscosity, surface tension, solid loading, and dispersion stability, are among the critical factors that determine the morphology and performance of a printed conductive pattern. The conductive ink in this work has a viscosity of 13.5 mPa s at a shear rate of 100 s^{-1} and a surface tension of 35 mN m^{-1} with a loading of 50 wt % metallic copper nanoparticles. The as-prepared copper-based conductive ink is stable for several weeks without any sedimentation. The other factors are the printing parameters, such as the pressure of the scraper, the printing speed, the screen mesh, etc. These factors require continuous groping and debugging in the test according to the size of the copper particles and ink formulations.

Another important factor that determines the performance of the printed electronics is the heat treatment of printed patterns, which can facilitate the removal of solvents and induce coalescence between copper particles.[26] The distinct annealing kinetics of the copper nanoparticles with different heat treatment temperatures are constrained by the characteristics of the particles, such as their size and melting point. Figure 8a–f shows SEM images of the copper patterns silk-screen printed on the polyimide substrates and annealed at different temperatures (150–250 °C) for 30 min under a nitrogen atmosphere. It can be readily discerned that the copper nanoparticles are uniform and independent of each other after being annealed at 150 °C. As the heat treatment temperature increases to 190 °C, adjacent nanoparticles start to melt and form small clusters. The small clusters partially connect with each other as the temperature reaches 190 °C (Figure 8c). As the sintering temperature increases to 250 °C, the particles completely interconnect with each other in a three-dimensional way, and in the meantime, significant coarsening occurs as the grain grows at the expense of the small copper particles. Also, the copper conductive patterns are densely compact, and no obvious cracks or voids are detected.

The microstructure of printed conductive patterns plays an important role in determining its electrical conductivity. Variations in electrical resistivity of the printed patterns as a function of heat treatment temperature are shown in Figure 9a.

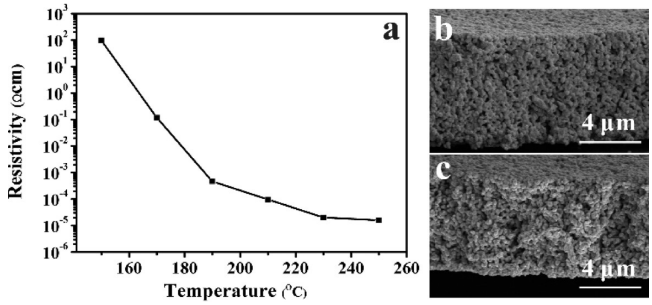

Figure 9. (a) Electrical resistivity of copper conductive patterns annealed at different temperatures. (b and c) Cross section SEM images of nanocopper conductive patterns sintered at 230 and 250 °C, respectively.

When the printed patterns were annealed at 150 °C under a nitrogen atmosphere for 30 min, most parts of the coarsened particles did not connect to each other and the measured resistivity was 98 Ω cm. As the annealing temperature increased from 150 to 190 °C, the resistivity was noticeably decreased from 98 Ω cm to 465 μΩ cm. The decrease in resistivity is probably due to the adjacent copper nanoparticles starting to melt and form small clusters with each other as shown in Figure 8. As the sintereing temperature reached 230 °C, the result resistivity decreased to 20.2 μΩ cm. It indicates that conduction paths between the copper particles are established via the melting of nanoparticles and the formation of interparticle connections. Especially when they are annealed at 250 °C, the copper particles completely interconnect with each other, which leads to the ideal resistance value of 15.8 μΩ cm. It indicates that a small amount of a protective agent layer on copper nanoparticles does not decrease the electrical resistivity

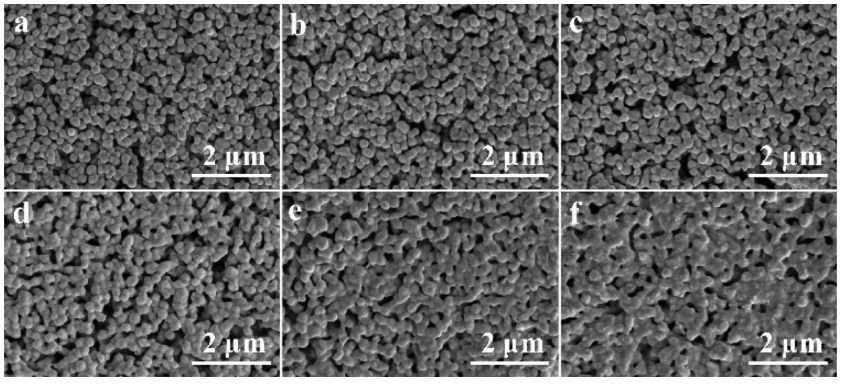

Figure 8. SEM images of the surface of nanocopper conductive ink on PI substrates with different annealing temperatures through silk-screen printing: (a) 150, (b) 170, (c) 190, (d) 210, (e) 230, and (f) 250 °C.

dx.doi.org/10.1021/am404620y | ACS Appl. Mater. Interfaces 2014, 6, 560–567

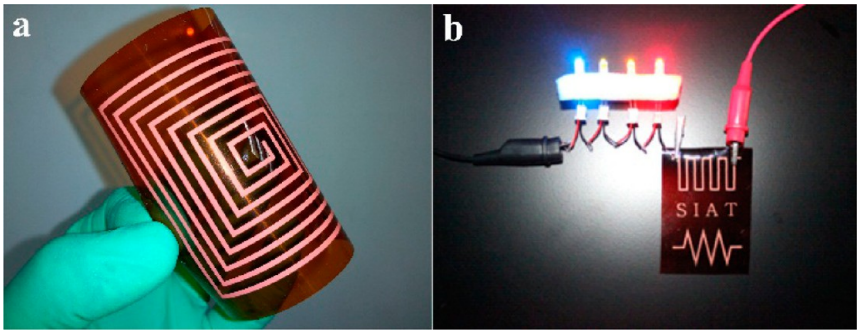

Figure 10. (a) Photograph of the bent printed copper pattern. (b) LED test connected with the printed copper pattern.

of the annealed copper pattern. Panels b and c of Figure 9 show the cross section SEM images of copper conductive patterns sintered at 230 and 250 °C, respectively. The thicknesses of the patterns sintered at 230 and 250 °C are 7.5 and 6.8 μm, respectively. No cracks in the patterns are observed. It is thus suggested that annealing leads to shrinkage in the z direction. This result clearly shows the annealing or melting point of the copper nanoparticles is significantly lower than that of bulk copper (1083 °C). The resistivity decreases gradually in the temperature range of 190−240 °C and becomes almost constant with a typical value of 15.8 $\mu\Omega$ cm after the temperature reaches 250 °C. This value is only 10 times larger than that of bulk copper (1.75 $\mu\Omega$ cm). It was reported that the resistivity of the conductive film based on 40−50 nm copper particles reached 17.2 $\mu\Omega$ cm with sintering at 325 °C for 1 h in vacuum.[26] Therefore, the annealing environment in our work is more suitable for application to organic flexible substrates like polyimide.

3.4. Manufacturing of Printed Copper Circuit Boards. Bendable electronic devices based on flexible substrates such as polyimide and epoxy resin have been attracting wide interest.[27,28] Generally, when the ink is converted into circuit patterns, the allowed annealing temperature is lower for flexible substrates because of their inherent low thermal durability. The temperature should be capable of achieving sintering to melt copper particles and completely remove the ink solvents, so that the copper nanoparticles could connect with each other to be conductive. As a result, the particle size of nanocopper, which affects its melting point and the formula of the conductive ink, determines the annealing conditions of the conductive pattern and also determines the choice of flexible organic substrates. To demonstrate the applicability of the synthesized copper-based conductive ink, the complex patterns were silk-screen printed onto specific flexible plastic substrates and then sintered at 250 °C for 30 min under an inert atmosphere. A continuous coil circuit with a 1 mm conductor width, a 2 mm conductor spacing, and a relatively uniform surface structure was manufactured (Figure 10a). The LED was integrated into a complete circuit with the printed copper patterns serving as a conducting wire, as shown in Figure 10b. A constant-voltage source provides a power supply for the circuit. The lighted LED demonstrated that the copper-printed circuit board worked. Test results indicate that the prepared nanocopper-based conductive ink in this work possesses good performance that can be employed in printed circuit boards for flexible printed electronics, such as organic light-emitting diodes, organic thin-film transistors, and solar cells. The copper-based conductive ink used here provides a convenient and low-cost method for fabricating conductive features.

4. CONCLUSIONS

We have synthesized copper nanoparticles with high monodispersivity, purity, and antioxidation in a cost-effective and eco-friendly polyol method. The obtained copper particles are phase-pure crystalline copper with *fcc* structure and could be stored in air for at least 30 days without being oxidized. The synthesized particles have an average size of 135 ± 30 nm, and the synthesis could be scaled up.

The copper nanoparticles can be well-dispersed in a mixed solvent to form a conductive ink with suitable viscosity and liquidity. When the copper conductive ink was silk-screen printed onto the flexible polyimide substrate, conductive copper patterns with a resistivity of 15.8 $\mu\Omega$ cm were achieved upon heat treatment at 250 °C for 30 min under an inert atmosphere. The optimal electrical resistivity is only 10 times larger than that of bulk copper, which is suitable for flexible printing electronics.

AUTHOR INFORMATION

Corresponding Authors

*E-mail: pl.zhu@siat.ac.cn.

*E-mail: rong.sun@siat.ac.cn.

Author Contributions

Y.Z. and P.Z. contributed equally to this work.

Notes

The authors declare no competing financial interest.

ACKNOWLEDGMENTS

This work was financially supported by the National Basic Research Program of China (973 Program) (2012CB933700-G), the National Natural Science Foundation of China (21101165), the Guangdong Innovative Research Team Program (2011D052 and KYPT20121228160843692), the Shenzhen Electronic Packaging Materials Engineering Laboratory (2012-372), the Shenzhen basic research plan (JC201005270372A, JC201005270366A, and JSGG20120615161915279), and the National S&T Major Project (2011ZX02709-001).

REFERENCES

(1) Perelaer, J.; Smith, P. J.; Mager, D.; Soltman, D.; Volkman, S. K.; Subramanian, V.; Korvink, J. G.; Schubert, U. S. *J. Mater. Chem.* **2010**, *20* (39), 8446−8453.

(2) Guo, R.; Yu, Y.; Xie, Z.; Liu, X.; Zhou, X.; Gao, Y.; Liu, Z.; Zhou, F.; Yang, Y.; Zheng, Z. *Adv. Mater.* **2013**, *25* (24), 3343−3350.

(3) Kim, D.; Jeong, S.; Moon, J. *Nanotechnology* **2006**, *17* (16), 4019−4024.

(4) Komoda, N.; Nogi, M.; Suganuma, K.; Otsuka, K. *ACS Appl. Mater. Interfaces* **2012**, *4* (11), 5732−5736.

(5) Wang, B. Y.; Yoo, T. H.; Song, Y. W.; Lim, D. S.; Oh, Y. J. *ACS Appl. Mater. Interfaces* **2013**, *5* (10), 4113−4119.
(6) Singh, M.; Haverinen, H. M.; Dhagat, P.; Jabbour, G. E. *Adv. Mater.* **2010**, *22* (6), 673−685.
(7) Perelaer, J.; Gans, B. J.; Schubert, U. S. *Adv. Mater.* **2006**, *18* (16), 2101−2104.
(8) Jang, S.; Cho, H.; Kang, S.; Oh, S.; Kim, D. *Appl. Phys. A: Mater. Sci. Process.* **2011**, *105* (3), 685−690.
(9) Yan, G. Q.; Wang, L.; Zhang, L. *Rev. Adv. Mater. Sci.* **2010**, *24*, 10−25.
(10) Dhas, N.; Raj, C.; Gedanken, A. *Chem. Mater.* **1998**, *10*, 1446−1452.
(11) Kumar, R. V.; Mastai, Y.; Diamant, Y.; Gedanken, A. *J. Mater. Chem.* **2001**, *11* (4), 1209−1213.
(12) Lee, J.; Kim, D.; Kang, W. *Bull. Korean Chem. Soc.* **2006**, *27*, 1869−1872.
(13) Sarkar, A.; Mukherjee, T.; Kapoor, S. *J. Phys. Chem. C* **2008**, *112*, 3334−3340.
(14) Zhang, H. X.; Siegert, U.; Liu, R.; Cai, W. B. *Nanoscale Res. Lett.* **2009**, *4* (7), 705−708.
(15) Casella, I.; Cataldi, T.; Guerrieri, A.; Desimoni, E. *Anal. Chim. Acta* **1996**, *335*, 217−225.
(16) Ohde, H.; Hunt, F.; Wai, C. *Chem. Mater.* **2001**, *13*, 4130−4135.
(17) Park, B. K.; Jeong, S.; Kim, D.; Moon, J.; Lim, S.; Kim, J. S. *J. Colloid Interface Sci.* **2007**, *311* (2), 417−424.
(18) Sun, J.; Jing, Y.; Jia, Y.; Tillard, M.; Belin, C. *Mater. Lett.* **2005**, *59* (29−30), 3933−3936.
(19) Magdassi, S.; Grouchko, M.; Kamyshny, A. *Materials* **2010**, *3* (9), 4626−4638.
(20) Yan, J.; Zou, G.; Hu, A.; Zhou, Y. N. *J. Mater. Chem.* **2011**, *21* (40), 15981−15986.
(21) Jeong, S.; Woo, K.; Kim, D.; Lim, S.; Kim, J. S.; Shin, H.; Xia, Y.; Moon, J. *Adv. Funct. Mater.* **2008**, *18* (5), 679−686.
(22) Lee, Y.; Choi, J. R.; Lee, K. J.; Stott, N. E.; Kim, D. *Nanotechnology* **2008**, *19* (41), 415604.
(23) Xiong, J.; Wang, Y.; Xue, Q.; Wu, X. *Green Chem.* **2011**, *13* (4), 900−904.
(24) Deng, D.; Jin, Y.; Cheng, Y.; Qi, T.; Xiao, F. *ACS Appl. Mater. Interfaces* **2013**, *5* (9), 3839−3846.
(25) Huang, H. H.; Yan, F. Q.; Kek, Y. M.; Chew, C. H.; Xu, G. Q.; Ji, W.; Oh, P. S.; Tang, S. H. *Langmuir* **1997**, *13*, 172−175.
(26) Park, B. K.; Kim, D.; Jeong, S.; Moon, J.; Kim, J. S. *Thin Solid Films* **2007**, *515* (19), 7706−7711.
(27) Lee, Y.-I.; Lee, K.-J.; Goo, Y.-S.; Kim, N.-W.; Byun, Y.; Kim, J.-D.; Yoo, B.; Choa, Y.-H. *Jpn. J. Appl. Phys.* **2010**, *49* (8), 086501.
(28) Lee, B.; Kim, Y.; Yang, S.; Jeong, I.; Moon, J. *Curr. Appl. Phys.* **2009**, *9* (2), e157−e160.